

Article

Change in the Properties of Expanded Polystyrene Exposed to Solar Radiation in Real Aging Conditions

Artur Nowoświat ¹, Artur Miros ² and Paweł Krause ^{1,*}

¹ Faculty of Civil Engineering, Silesian University of Technology, 44-100 Gliwice, Poland; artur.nowoswiat@polsl.pl

² ŁUKASIEWICZ Research Network-Warsaw Institute of Technology, 3 Duchnicka Street, 01-796 Warszawa, Poland; artur.miros@wit.lukasiewicz.gov.pl

* Correspondence: pawel.krause@polsl.pl

Abstract: Although polystyrene materials with added graphite are actively used for the thermal insulation of buildings, there are serious problems with the detachment and warping of these materials under the influence of solar radiation. However, no systematic studies have yet been carried out on the aging of polystyrene under exposure to solar radiation. The article presents research aimed at determining changes in the thermal conductivity, compressive stress, tensile strength, and water absorption of expanded polystyrene with the addition of graphite, exposed to direct solar radiation under in situ conditions. For this purpose, expanded polystyrene (EPS) with the addition of graphite (gray EPS) and expanded polystyrene made of composite panels (gray EPS and white EPS) were exposed to direct solar radiation under in situ conditions. A third sample (reference), which was entirely white polystyrene (without the addition of graphite), was included in the tests. The results showed that expanded polystyrene with the addition of graphite degraded under the influence of direct solar radiation but improved its strength properties. Expanded polystyrene made of composite improved its compressive strength properties by nearly 11 kPa (18%), and expanded polystyrene with the addition of graphite improved its compressive strength properties by 0.4 kPa (0.5%). And the tensile strength for composite-made expanded polystyrene increased by 7 kPa (9%), and that for expanded polystyrene with the addition of graphite increased by 26 kPa (37%). At the same time, water absorption for expanded polystyrene made of composite also increased by 0.06 kg/m² (60%), and that for expanded polystyrene with the addition of graphite increased by 0.04 kg/m² (44%).

Keywords: expanded polystyrene (EPS); gray polystyrene; sun; strain; strength; absorption



Citation: Nowoświat, A.; Miros, A.; Krause, P. Change in the Properties of Expanded Polystyrene Exposed to Solar Radiation in Real Aging Conditions. *Sustainability* **2024**, *16*, 7320. <https://doi.org/10.3390/su16177320>

Academic Editor: Antonio Caggiano

Received: 27 June 2024

Revised: 30 July 2024

Accepted: 18 August 2024

Published: 26 August 2024



Copyright: © 2024 by the authors. Licensee MDPI, Basel, Switzerland. This article is an open access article distributed under the terms and conditions of the Creative Commons Attribution (CC BY) license (<https://creativecommons.org/licenses/by/4.0/>).

1. Introduction

A significant part of building materials have insufficient thermal insulation properties, leading to a significant increase in global energy consumption and carbon dioxide emissions in the housing sector [1,2]. As described in the literature, the construction industry is responsible for more than 40% of global energy consumption and 56.7% of carbon dioxide emissions [3,4]. Insulating materials used in construction should help protect the climate, which is one of the most important issues in the modern world [5,6]. Thermal insulation is a material or combination of materials that, when properly applied, reduces heat losses that occur through conduction, convection, and radiation [7]. As a rule, such materials are environmentally friendly and extend the periods of thermal comfort in rooms, and apart from other advantages, they reduce noise levels or increase fire protection [8]. Sustainable insulation products with lower embodied energy and reduced environmental emissions are increasingly popular, and a large number of innovative types of insulation are constantly entering the market [9]. Conventional materials preferred in construction due to the use of thermal energy storage and due to their low thermal conductivity and low cost include polyurethane (PUR), polyisocyanurate (PIR), extruded polystyrene (XPS), and expanded

polystyrene (EPS) [10]. These materials affect both the thermal accumulation capacity of walls and their thermal insulation. Insulating materials provide high thermal resistance by reducing the rate of heat flow [8,11]. In many works in recent years, it has been observed that thermal conductivity is a function of factors such as humidity, temperature, and density [12–14].

One of the commonly used materials is expanded polystyrene (EPS), which, due to the 98% air content, has a fairly low density in the range of 20–30 kg/m³ [15–17].

The literature offers research studies on changes in the effective thermal conductivity of insulating materials after rapid aging by exposing them to elevated temperatures, relatively high humidity, and freeze–thaw cycles [12], as well as their flammability [18,19]. We can also find studies on the effect of sunlight on polystyrene with the addition of graphite (gray EPS) [20]. Currently, expanded polystyrene with the addition of graphite is commonly used for thermal insulation. The effectiveness of its use was confirmed by Lakatos et al. [21], who tested five different graphite-enhanced polystyrene insulations. The authors concluded that each of the tested materials had different water absorption and thermal insulation properties, which may have been due to differences in the manufacturing process. There are many works on the use of a life cycle approach in the analysis of insulating materials [22–24]. When analyzing the life cycle, we cannot ignore the influence of solar radiation on the properties of insulating materials.

In an earlier work by the authors of this article [20], the material exposed to solar radiation was tested under laboratory conditions. This article presents the results of tests of the material exposed to solar radiation under real conditions over a period of 4 years.

2. Methodology

The subject of the tests involved three EPS boards with a thickness of 0.15 m and dimensions of 0.5 m by 1.0 m, labeled board A, board B, and board C.

This small number of samples was dictated by the small available research site in situ and the duration of the investigation (4 years). Taking into account this fact and the fact that the polystyrene used for testing was typical, i.e., the batches of material did not differ significantly from each other, a decision was made to use the minimum number of samples.

Board A—Board A consisted of composite polystyrene consisting of two layers—the main one in the form of gray expanded polystyrene and the additional one with a thickness of 0.006 m in the form of white expanded polystyrene (the layer protecting the gray layer against solar radiation). Samples were numbered as follows:

- 2—Sample before exposure to solar radiation;
- 5—Sample after exposure to solar radiation.

Board B—Board B consisted of a polystyrene board made entirely of expanded polystyrene with graphite content (gray polystyrene). Samples were numbered as follows:

- 3—Sample before exposure to solar radiation;
- 6—Sample after exposure to solar radiation.

Board C—Board C consisted of expanded polystyrene without the addition of graphite (white polystyrene) with enhanced technical parameters. Samples were numbered as follows:

- 1—Sample before exposure to solar radiation;
- 4—Sample after exposure to solar radiation.

The polystyrene boards remained glued to the wall surface for 4 years. At that time, they were not protected or shielded against the adverse effects of external environment conditions in any way.

2.1. Emissivity of the Boards

The emissivity of the boards has already been determined in the preliminary research carried out by the authors of this article [25].

For the tests under real conditions, the following were used:

- A thermal imaging camera (Teledyne FLIR LLC 27700 SW Parkway Ave, Wilsonville, OR, USA) with a temperature measurement range of $-20\text{ }^{\circ}\text{C} \pm 1500\text{ }^{\circ}\text{C}$, resolution of 161,472 pixels, thermal sensitivity for the lens of $42^{\circ} \times 32^{\circ} < 30\text{ mK}$, IFOV spatial

resolution of 2.41 mrad/pixel for the lens $42^\circ \times 32^\circ$, and segmental spectral sensitivity of 7.5–14 μm ;

- The VantagePro2 meteorological station (Davis Instruments, Hayward, CA, USA) with the temperature measurement range of $-40^\circ\text{C} \div 65^\circ\text{C} \pm 0.5^\circ\text{C}$, humidity of $1\% \div 100\% \pm 3\%$, and solar radiation intensity of $0\text{--}1999\text{ W/m}^2 \pm 1\text{ W/m}^2$.

The station consisted of a console connected to an integrated set of ISS sensors, which included temperature sensors.

The tests were carried out on a stationary in situ test stand, which was located in a place with the geographical coordinates $18^\circ 54'$ E, $50^\circ 10'$ N. The tested expanded polystyrene boards were glued to the wall with southern exposure to solar radiation using a dedicated polyurethane adhesive (Figure 1) [25].



Figure 1. View of the facade panels on the test stand.

2.2. Thermal Conductivity Measurements

The study was carried out according to the following procedure:

1. For the sample preparation, a sample of 600×600 was prepared from a board with dimensions of $1000 \times 500 \times 1500$ mm. The test sample consisted of three parts, 600×500 mm, 500×100 mm, and 100×100 mm.

2. Conditioning occurred at a room temperature of $(23 \pm 2)^\circ\text{C}$ and a relative humidity of $(50 \pm 5)\%$ for at least 14 days.

3. Measurements were carried out according to the EN 12667 standard [26].

The apparatus was the FOX 600 by LaserComp (LASERCOMP, INC., Wakefield, MA, USA).

2.3. Measurements of Compressive Stress

The study was carried out according to the following procedure:

1. For the sample preparation, 3 samples of 150 × 150 × 150 mm were prepared from a board with dimensions 1000 × 500 × 1500 mm. Samples exposed to weather conditions were cut from a board with dimensions of 500 × 500 × 150 mm.
2. Conditioning occurred in normal conditions for at least 14 days.
3. For pretension of (50 ± 5) Pa, the test continued until the sample deformed 10%.

The used equipment was the Matest 20kN MATEST Service testing machine (MATEST S.p.A. Viale Mantegna, Ascore, Italy) [27], wherein

$$\sigma_{10} = \frac{F_{10}}{A_0} \cdot 10^3, \quad (1)$$

where F_{10} is a force corresponding to 10% of the strain [N] and A_0 is the initial surface area of the sample (100 × 100) mm [mm²].

The test was carried out at a temperature of (23 ± 5) °C.

2.4. Tensile Strength Measurements

The study was carried out according to the following procedure:

1. For the sample preparation, 3 samples of 150 × 150 × 150 mm were prepared from a board with dimensions 1000 × 500 × 1500 mm. Samples exposed to weather conditions were cut from a board with dimensions of 500 × 500 × 150 mm.
2. Conditioning occurred at a room temperature of (23 ± 2) °C and a relative humidity of (50 ± 5)% for at least 14 days.
3. For pretension of (10 ± 1) mm/min, the test continued until the sample deformed 10%.

The used equipment was the Matest 20kN MATEST Service testing machine [28], wherein

$$\sigma_{mt} = \frac{F_m}{A_0} \cdot 10^3, \quad (2)$$

where F_m is the maximum tensile force [kN] and A_0 is the surface area of the sample (100 × 100) mm [mm²].

The test was carried out at a temperature of (23 ± 5) °C.

2.5. Water Absorption Measurements

The study was carried out according to the following procedure:

1. For the sample preparation, 4 samples with dimensions of 100 × 100 mm were cut from an EPS board with dimensions of 1000 × 500 mm.
2. Conditioning occurred under normal conditions for at least 14 days.
3. The test was carried out in accordance with the standard EN 1607 [28].

Water absorption at long-term partial immersion W_{lp} was defined as

$$W_{lp} = \frac{m_{28} - m_0}{A_p}, \quad (3)$$

where m_0 is the sample weight before testing [kg], m_{28} is the weight of the sample after 28 days of partial immersion in water [kg], and A_p is the bottom surface of the sample immersed in water [m²].

3. Results and Discussion

The results of climate measurements are presented graphically. The research was carried out as continuous measurements using the local meteorological station VantagePro2 Davis Instruments. The outside air temperature was measured at a height of 200 cm above ground level. The measurement started at 0:00 on 1 September, 2018, and ended on 13 October, 2022, at 7:00. The findings were recorded every 10 min as a ten-minute average. A total of 204,008 measurement results were recorded. During the first full measurement period (from August to July of the following year), the minimum external temperature

$t_{e \min} = -10.8 \text{ }^{\circ}\text{C}$ and the highest $t_{e \max} = +36.9 \text{ }^{\circ}\text{C}$ were recorded. The following year was characterized by the lowest temperature amplitude. In winter, the minimum temperature was $t_{e \min} = -6.9 \text{ }^{\circ}\text{C}$, and the highest was $t_{e \max} = +32.7 \text{ }^{\circ}\text{C}$. The third measurement year was characterized by the lowest temperature during the investigation, which was $t_{e \min} = -16.2 \text{ }^{\circ}\text{C}$. The highest temperature was $t_{e \max} = +33.8 \text{ }^{\circ}\text{C}$. In the last year, no extreme temperature values were recorded either in summer or winter. Figure 2 shows the results of the outdoor air temperature measurement.

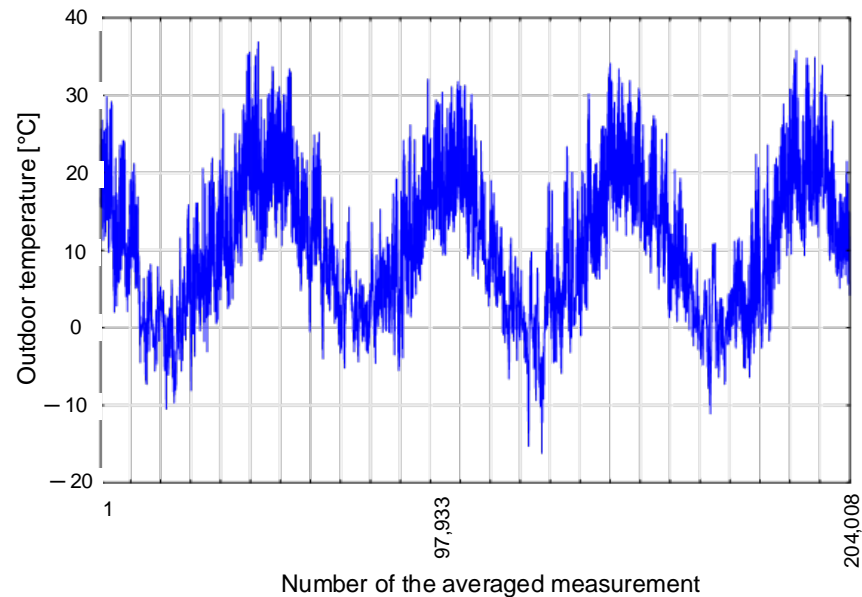


Figure 2. Temperature distribution over 4 years.

Measurements of the intensity of solar radiation were also performed in the horizontal plane (Figure 3). In the case of the impact of solar radiation intensity, in the first year of the study, the highest number of hours with an intensity ranging from 600 to 1000 W/m^2 was recorded. The fewest number of days with the intensity exceeding 600 W/m^2 was recorded in the second year, despite the occurrence of its local maximum values throughout the entire measurement period.

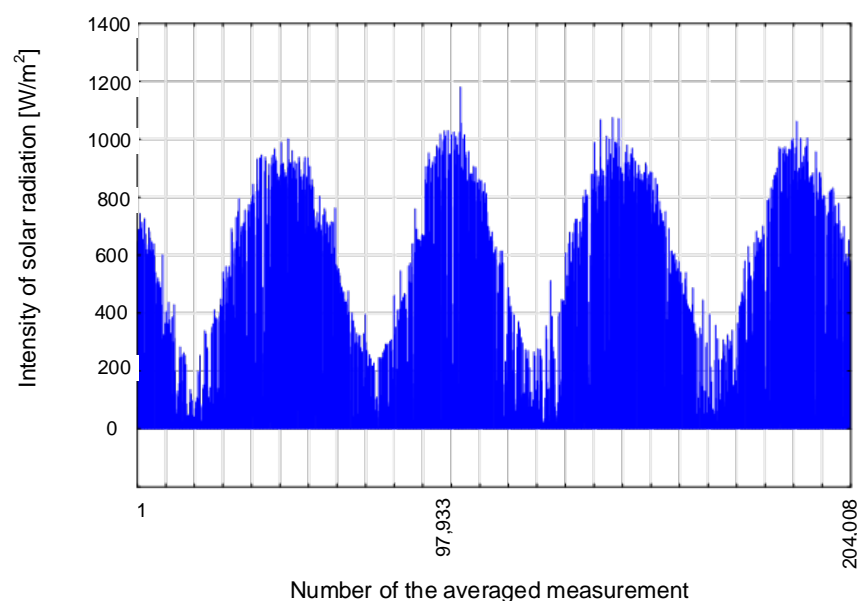


Figure 3. Distribution of solar radiation onto the horizontal plane over a period of 4 years.

In situ research was based mainly on thermal imaging measurements. Measurement elements in the form of measurement points (Sp), measurement lines (Li), and rectangular areas (Bx) were applied to the thermal images of the analyzed objects. An exemplary thermogram of the measurements is shown in Figure 4. The highest measured temperature on the thermal insulation surface exceeded 80 °C for board B. Much lower maximum temperatures were recorded for board A, slightly exceeding 40 °C. Board C was characterized by a surface temperature lower than max. 6 °K compared with board A. The temperature distribution within the individual polystyrene boards was, of course, dependent on the speed of the acting wind. This was especially visible on the surface of board B (Figure 4). The impact of the wind caused dynamic temperature changes that were recorded in a thermal imaging camera and presented on a thermogram in the form of the so-called heat plume. In the case of plates A and C, local point growths in temperature were observed in the thermograms. They were related to small inclusions of single graphite polystyrene granulates and, in the case of board A, to the penetration of the graphite polystyrene layer under partially melted white polystyrene balls (a layer of small thickness). However, such situations occurred relatively rarely (Figure 1). The expanded polystyrene boards were subjected to the non-uniform influence of solar radiation because of the proximity of the surrounding objects. This resulted in the presence of shading at certain times of the day (Figure 5). This resulted in temperature differences within the graphite polystyrene board exceeding 30 °K during periods of exposure to high-intensity solar radiation. This uneven heating of the polystyrene boards may consequently lead to their partial deformation.

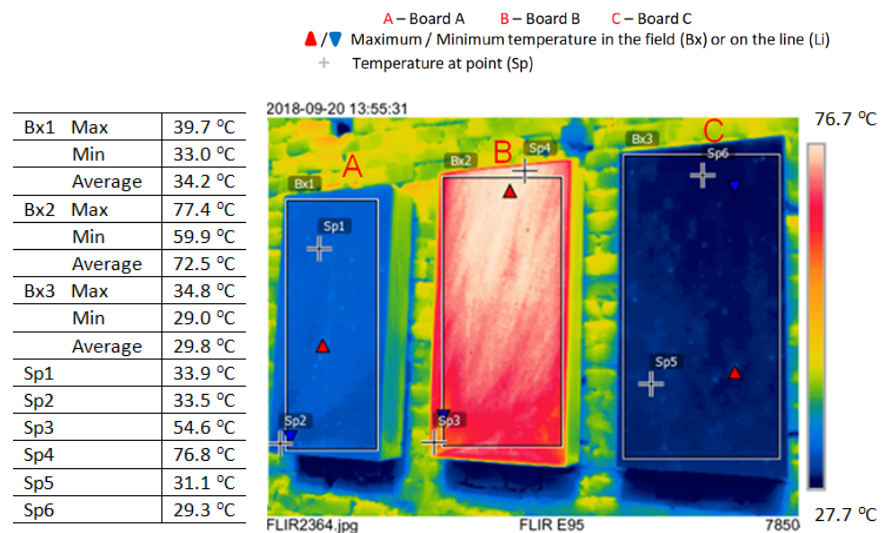


Figure 4. Exemplary measurement of temperature distribution on the surface of three panels when exposed to direct solar radiation.

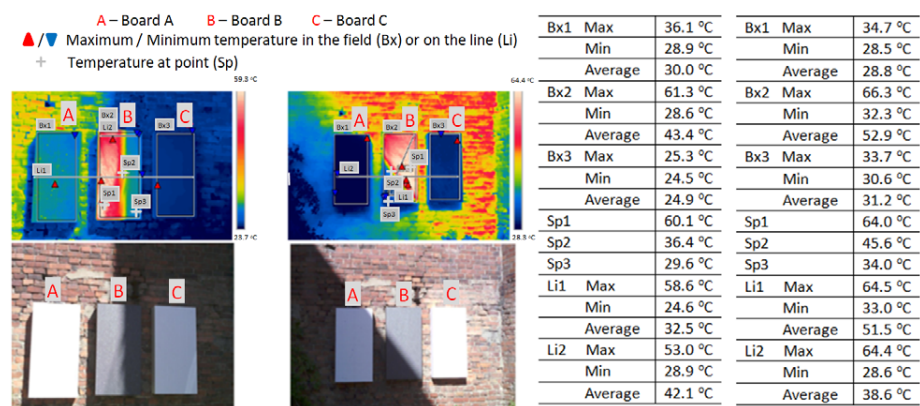


Figure 5. Thermograph demonstrated in different shading conditions.

First, for EPS samples, which were subjected to aging at a later stage, the thermal conductivity coefficient was determined by means of measurements (Table 1).

Table 1. Thermal conductivity coefficient of the boards.

Sample Type	Sample Thickness, mm	Thermal Conductivity Coefficient, W/mK
Sample A	149.40	0.03061
Sample B	149.64	0.03060
Sample C	149.41	0.03930

The thermal conductivity coefficient for samples after aging was not determined, because the measurement in the HFM or GHP plate apparatus should be performed on samples with flat parallel surfaces, without air voids (gaps, pits, or holes) between the apparatus plates and the sample surface. The lack of flat parallelism causes the contact resistance to be unevenly distributed between the sample and the working surfaces of hot and cold plates and the thermal flux density sensor of the apparatus. This causes an inhomogeneous heat flux distribution and distortion of the thermal field inside the sample. Therefore, accurate surface temperature measurements are difficult to obtain. In the samples taken from the facade of the building, the surfaces contained a significant number of holes, especially on the side exposed to solar radiation, and there was also no surface parallelism required to measure the thermal conductivity coefficient. Eliminating those surface inaccuracies by cutting off, e.g., 1–2 cm of the layer would have removed the part of the material that had undergone the greatest changes during the aging process.

The other test results were related to performance under compression conditions. Each of the samples tested was cube-shaped with a side length of 0.15 m.

Three compressive stress measurements were obtained for each sample. The measurement result was defined as the average with standard uncertainty. The results of the compression stress at 10% stress are shown in Table 2.

Table 2. Compressive stress results.

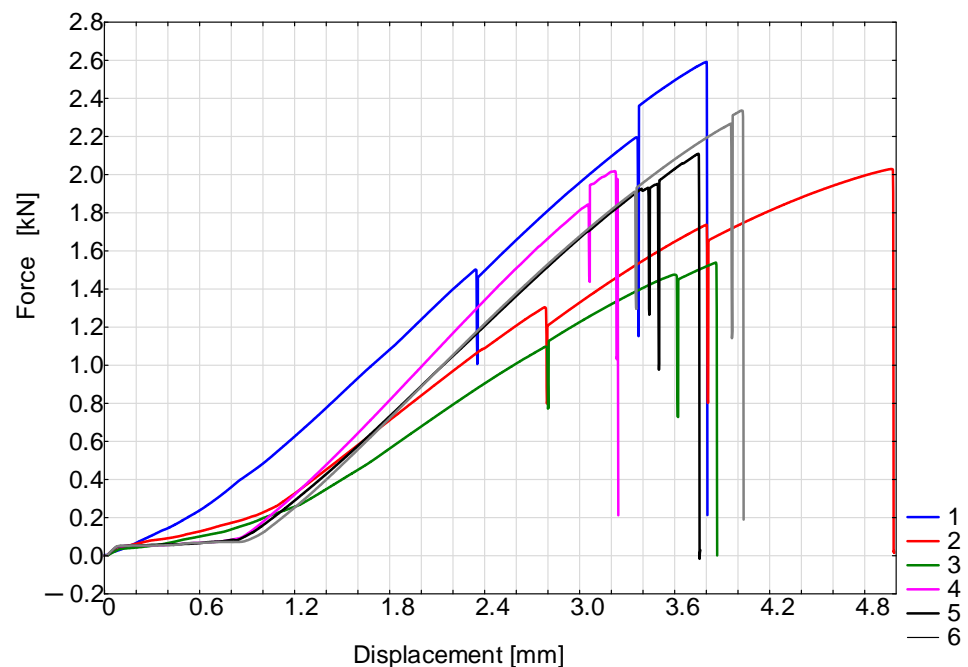
Sample Type	Sample Number	Compressive Stress at 10% Strain, kPa	Standard Uncertainty
Sample A	2	60.9	4.59
	5	71.3	3.13
Sample B	3	67.9	3.42
	6	68.2	0.854
Sample C	1	90.6	3.10
	4	77.2	0.874

The results obtained (Table 2) indicate that white polystyrene (sample C) had the best properties because the greatest force must be used to compress it by 10% of the initial value. It could also be seen that this polystyrene, as the only one among the tested ones, lost a lot in terms of compressive stress, although the value of 77.2 kPa was still the highest. Gray polystyrene (sample B) had the worst properties. It should also be noted that gray polystyrene (sample B) and gray polystyrene with a white polystyrene lining (sample A) improved their properties in terms of strains. This was probably due to the fact that solar radiation melted the samples so much that the structure became more consolidated, which affected the compressive strength. The next results concerned the determination of the tensile strength perpendicular to the front surfaces. The tested specimens were cube-shaped with dimensions of 0.15 m. The results are presented in Table 3.

Table 3. Tensile strength results.

Sample Type	Sample Number	σ_{mt} , kPa	Standard Uncertainty
Sample A	2	82	15
	5	89	4.2
Sample B	3	70	14
	6	96	10
Sample C	1	96	23
	4	84	9.8

The results indicated that on average, sample C (white polystyrene) prior to the aging process had the best tensile strength properties. And after the aging process, the decrease in tensile strength was significant and reached a value lower than that of other samples, which demonstrated significantly higher tensile strength after aging. The interpretation of this finding may be similar to that of the compressive stress test (Figure 6).

**Figure 6.** Damage diagrams of the tested samples.

The last parameter tested was water absorption. The results of this study are presented in Table 4.

Table 4. Water absorption results of the tested samples.

Sample Type	Sample Number	Water Absorption, kg/m ²	Standard Uncertainty
Sample A	2	0.10	0.033
	5	0.16	0.034
Sample B	3	0.09	0.048
	6	0.13	0.084
Sample C	1	0.23	0.094
	4	0.19	0.047

Based on Table 4, it can be concluded that for samples A and B (containing graphite), the absorption of water after aging resulting from exposure to solar radiation increased. For sample C (white polystyrene), this effect was the opposite. This may be due to the fact that solar exposure degraded samples with graphite admixture more than without it.

4. Conclusions

The test results demonstrated that the influence of solar radiation under in situ conditions on the unprotected samples of the three types of expanded polystyrene was significant. Indisputably, gray polystyrene (sample B) had the best thermal insulation properties. The thermal conductivity coefficient of the tested sample was 0.03061 W/mK. Slightly lower thermal insulation properties were demonstrated by a composite panel (sample A) with a top layer of white polystyrene. The lowest thermal insulation properties were found for white polystyrene (sample C).

1. Despite the 4-year impact of external environmental conditions on the unprotected surfaces of the thermal insulation materials tested, there was no significant change in the thickness of the tested EPS boards. The damage that occurred (holes or polystyrene melting) was merely local and uneven (random?). As a consequence, they did not cause significant deterioration of the thermal resistance related to the reduction in their thickness as a result of ongoing aging processes. It can be assumed that the dynamics of changes related to the reduction in the polystyrene thickness were not constant and changed over time. This has been demonstrated by examples of unprotected polystyrene exposed to weather conditions for a dozen or so years.
2. In addition, under the influence of degradation, expanded polystyrene with an admixture of graphite (samples A and B) improved its compressive and tensile strength properties. This may be due to the degradation manner of this material, where the polystyrene balls stuck together, creating a homogeneous structure (without air). Of course, the increase in strength did not fully compensate for the effects of such deformations.
3. Definitely, the negative effect of direct exposure of expanded polystyrene with the addition of graphite (samples A and B) was attributed to an increase in water absorption of up to 50% (Table 4). This effect was not found for white polystyrene (sample C). Despite the increase in the strength of samples A and B resulting from exposure to direct solar radiation, such measures were not recommended.
4. Gray polystyrene (sample B) after direct exposure to solar radiation deformed so much that the increase in its compressive or tensile strength did not compensate for the losses resulting from the boards falling off the building facade.
5. It should be noted that the composite panel (sample A) improved its strength properties, but its protection with a white coating on the side exposed to radiation may indicate that there was no significant stress. Such studies are planned in the future and may yield positive results for such panels.

Although the conclusions are generally well supported, it is important to emphasize that direct solar radiation is not recommended for EPS, as it can lead to deformation and other negative effects. Additional research into potential protective coatings or other mitigating measures would be beneficial.

However, in summary, it should be noted that despite the problems indicated in this article, the advantage of this material involves its positive impact on sustainable development in construction. Namely, foamed polypropylene fluidizes under the influence of heat and then hardens during cooling in a reversible process. Therefore, it can be recycled for an unlimited period of time.

Author Contributions: Conceptualization, A.N. and P.K.; methodology, P.K. and A.M.; validation, A.N.; formal analysis, A.N.; investigation, A.N., P.K. and A.M.; resources, P.K. and A.M.; data curation, A.N.; writing—original draft preparation, A.N.; writing—review and editing, A.N.; visualization, A.N. and P.K.; supervision, A.N.; project administration, A.N. and P.K. All authors have read and agreed to the published version of the manuscript.

Funding: This research received no external funding.

Institutional Review Board Statement: Not applicable.

Informed Consent Statement: Not applicable.

Data Availability Statement: The data are held by the author and will be made available at the request of the interested party.

Acknowledgments: The article was written as part of Artur Nowoświat's scientific internship at LUKASIEWICZ Research Network-Warsaw Institute of Technology, under the supervision of Artur Miros.

Conflicts of Interest: The authors declare no conflicts of interest.

References

1. Benchouia, H.E.; Boussehel, H.; Guerira, B.; Sedira, L.; Tedeschi, C.; Becha, H.E.; Cucchi, M. An experimental evaluation of a hybrid biocomposite based on date palm petiole fibers, expanded polystyrene waste, and gypsum plaster as a sustainable insulating building material. *Constr. Build. Mater.* **2024**, *422*, 135735. [\[CrossRef\]](#)
2. Mahmoodzadeh, M.; Gretka, V.; Blue, A.; Adams, D.; Dallimore, B.; Mukhopadhyaya, P. Evaluating thermal performance of vertical building envelopes: Case studies in a Canadian university campus. *J. Build. Eng.* **2021**, *40*, 102712. [\[CrossRef\]](#)
3. Hung Anh, L.D.; Pásztor, Z. An overview of factors influencing thermal conductivity of building insulation materials. *J. Build. Eng.* **2021**, *44*, 102604. [\[CrossRef\]](#)
4. Patil, S.B.N.; Jaiswal, T.P.; Selvakumar, K.K.; Jyothi, M.S.; Jyothilakshmi, R.; Kumar, S. Development of sustainable alternative materials for the construction of green buildings using agricultural residues: A review. *Constr. Build. Mater.* **2023**, *368*, 130457.
5. Berardi, U.; Sprengard, C. An overview of and introduction to current researches on super insulating materials for high-performance buildings. *Energy Build.* **2020**, *214*, 109890. [\[CrossRef\]](#)
6. Krause, P.; Nowoświat, A.; Pawłowski, K. The impact of international insulation on heat transport through the wall: Case Study. *Appl. Sci.* **2020**, *10*, 7484. [\[CrossRef\]](#)
7. ASHRAE HVAC 2001 Fundamentals Handbook 2001 (SI). In *American Society of Heating Refrigerating & Air Conditioning Engineers Incorporated*; Elsevier: Amsterdam, The Netherlands, 2001.
8. Al-Homoud, M.S. Performance characteristics and practical applications of common building thermal insulation materials. *Build. Environ.* **2005**, *40*, 353–366. [\[CrossRef\]](#)
9. Walker, R.; Pavia, S. Thermal performance of a selection of insulation materials suitable for historic buildings. *Build. Environ.* **2015**, *94*, 155–165. [\[CrossRef\]](#)
10. Villasmil, W.; Fischer, L.J.; Worlitschek, J. A review and evaluation of thermal insulation materials and methods for thermal energy storage systems. *Renew. Sustain. Energy Rev.* **2019**, *103*, 71–84. [\[CrossRef\]](#)
11. Khoukhi, M.; Abdelbagi, S.; Hassan, A.; Darsaleh, A. Impact of dynamic thermal conductivity change of EPS insulation on temperature variation through a wall assembly. *Case Stud. Therm. Eng.* **2021**, *25*, 100917. [\[CrossRef\]](#)
12. Berardi, U. The impact of aging and environmental conditions on the effective thermal conductivity of several foam materials. *Energy* **2019**, *182*, 777–794. [\[CrossRef\]](#)
13. Winkler-Skalna, A.; Łoboda, B. Determination of the thermal insulation properties of cylindrical PUR foam products throughout the entire life cycle using accelerated aging procedures. *J. Build. Eng.* **2020**, *31*, 101348. [\[CrossRef\]](#)
14. Orlik-Koźdoń, B.; Nowoświat, A. Modelling and testing of a granular insulating material. *J. Build. Phys.* **2018**, *42*, 6–15. [\[CrossRef\]](#)
15. Kaya, A.; Kar, F. Properties of concrete containing waste expanded polystyrene and natural resin. *Constr. Build. Mater.* **2016**, *105*, 572–578.
16. Lu, J.; Wang, D.; Jiang, P.; Zhang, S.; Chen, Z.; Bourbigot, S.; Fontaine, G.; Wei, M. Design of fire resistant, sound-absorbing and thermal-insulated expandable polystyrene based lightweight particleboard composites. *Constr. Build. Mater.* **2021**, *305*, 124773. [\[CrossRef\]](#)
17. Sulong, N.H.R.; Mustpa, S.; Rashid, M. Application of expanded polystyrene (EPS) in buildings and constructions: A review. *J. Appl. Polym. Sci.* **2019**, *136*, 47529. [\[CrossRef\]](#)
18. Li, L.; Chen, S.; Wang, S.; Tao, X.; Zhu, X.; Cheng, G.; Gui, D. Influence of pickling on the surface composition and flotability of Daliuta long-flame coal. *Powder Technol.* **2019**, *352*, 413–421. [\[CrossRef\]](#)
19. Tang, L.; Chen, S.; Wang, S.; Tao, X.; He, H.; Zheng, L.; Ma, C.; Zhao, Y. Heterocyclic sulfur removal of coal based on potassium tert-butoxide and hydrosilane system. *Fuel Process. Technol.* **2018**, *177*, 194–199. [\[CrossRef\]](#)
20. Nowoświat, A.; Krause, P.; Miros, A. Properties of expanded graphite polystyrene damaged by the impact of solar radiation. *J. Build. Eng.* **2021**, *34*, 101920. [\[CrossRef\]](#)
21. Lakatos, Á.; Kalmár, F. Investigation of thickness and density dependence of thermal conductivity of expanded polystyrene insulation materials. *Mater. Struct.* **2013**, *46*, 1101–1105. [\[CrossRef\]](#)
22. Ricciardi, P.; Belloni, E.; Cotana, F. Innovative panels with recycled materials: Thermal and acoustic performance and life cycle assessment. *Appl. Energy* **2014**, *134*, 150–162. [\[CrossRef\]](#)
23. Biolek, V.; Hanák, T. LCC Estimation Model: A construction material perspective. *Buildings* **2019**, *9*, 182. [\[CrossRef\]](#)
24. Gomes, R.; Silvestre, J.D.; de Brito, J. Environmental life cycle assessment of thermal insulation tiles for flat roofs. *Materials* **2019**, *12*, 2595. [\[CrossRef\]](#)
25. Krause, P.; Nowoświat, A. Experimental studies involving the impact of solar radiation on the properties of expanded graphite polystyrene. *Energies* **2020**, *13*, 75. [\[CrossRef\]](#)

26. *EN 12667:2001*; Thermal Performance of Building Materials and Products—Determination of Thermal Resistance by Means of Guarded Hot Plate and Heat Flow Meter Methods—Products of High and Medium Thermal Resistance. European Committee for Standardization: Brussels, Belgium, 2001.
27. *EN 826*; Thermal Insulating Products for Building Applications—Determination of Compression Behavior. European Committee for Standardization: Brussels, Belgium, 2013.
28. *EN 1607*; Thermal Insulating Products for Building Applications—Determination of Tensile Strength Perpendicular to Faces. European Committee for Standardization: Brussels, Belgium, 2013.

Disclaimer/Publisher’s Note: The statements, opinions and data contained in all publications are solely those of the individual author(s) and contributor(s) and not of MDPI and/or the editor(s). MDPI and/or the editor(s) disclaim responsibility for any injury to people or property resulting from any ideas, methods, instructions or products referred to in the content.